Lab on a Chip

Cite this: *Lab Chip*, 2011, **11**, 4260

www.rsc.org/loc

PAPER

A new method of UV-patternable hydrophobization of micro- and nanofluidic networks

Rerngchai Arayanarakool, Lingling Shui, Albert van den Berg and Jan C. T. Eijkel*

Received 2nd August 2011, Accepted 29th September 2011
DOI: 10.1039/c1lc20716d

This work reports a new method to hydrophobize glass-based micro- and nanofluidic networks. Conventional methods of hydrophobizing glass surfaces often create particulate debris causing clogging especially in shallow nanochannels or require skilful handling. Our novel method employs oxygen plasma, silicone oil and ultraviolet (UV) light. The contact angle of the modified bare glass surface can reach 100° whilst the inner channels after treatment facilitate stable and durable water-in-oil droplet generation. This modified surface was found to be stable for more than three weeks. The use of UV in principle enables in-channel hydrophobic patterning.

1. Introduction

Droplet-based microfluidics is one of the most promising tools in the microfluidic system since its monodisperse, well-confined and precisely controlled droplets can be used as tiny compartmentalized carriers for both bio- and chemical reactions and analyses.[1–11] Depending on the surface properties of the material of a chip, the emulsion can be formed as either water-in-oil (W/O) or oil-in-water (O/W) facilitating different usages,[12] for instance, the encapsulation of cells in water droplets in the oil phase[13–17] or the polymerization of microparticles from the emulsion of non-polar droplets with dissolved monomers in the water phase.[18–23] In general, polydimethylsiloxane (PDMS)-based microfluidic devices are widely used to generate W/O emulsions.[24–33] However, their intrinsic properties *i.e.* oil adsorption,[34–36] gas and small-molecule permeability,[37,38] roof collapse,[39–42] and low bonding strength inhibit their usage especially in nanofluidic devices. Alternatively, glass-based microfluidic devices can be used after chemical hydrophobization by silanization *i.e.* perfluorodecyltrichlorosilane (FDTS)[43–46] and octadecyltrichlorosilane (ODS).[47–50] However, these chemicals are quite reactive to oxygen or water in air causing the formation of particulate debris in the shallow channels. The modification operation must therefore be skillfully handled under nitrogen atmosphere or water-free condition in the case of FDTS or ODS depositions, respectively, and even then particle formation often occurs. Especially the intersections of micro- and nanochannels are critical areas for particulate clogging.

In addition, hydrophobic patterning is a promising technique applicable to various lab-on-a-chip devices for example to create hydrophobic valves,[51–53] cellular or biomolecular attachment[54,55] and so on. However, almost all the modification approaches are successfully performed on a plane wafer before bonding but not in the enclosed system, and in-channel hydrophobic patterning approaches have been rarely reported. Zhao *et al.*[51] proposed two approaches to pattern hydrophobic surfaces in the enclosed microfluidic system. In the first approach, they utilized multi-stream laminar flows of silane solution and solvent to pattern a hydrophobic area in a glass-based microchannel network. However, this method was limited by the preformed channel networks. Alternatively, in the second approach, the hydrophobic surface was initially formed by photocleavable self-assembly monolayers with 2-nitrobenzyl groups prior to UV irradiation through a photomask to pattern the hydrophilic region. However, it still required several steps to perform the photolithography.

Vong *et al.*[55] proposed an alternative approach to pattern hydrophobic sites inside a fused silica capillary tube using trifluoroethyl undec-10-enoate (TFEE) with 10 hour UV exposure. A TFEE molecule was used to create a hydrophobic surface with high surface coverage due to less steric hindrance and could also be used as a linker for further surface coupling with primary amines. Even though this method provided patterned hydrophobization with high surface coverage and the opportunities for further surface coupling, it took quite a long time (10 h) to achieve the whole procedure.

Here we propose a novel approach to hydrophobize glass surfaces inside closed channels which is suitable for micro- and nanochannel networks in which the intersections of micro- and nanochannels are critical areas for particulate clogging. Furthermore, this method allows easy patterning of the surface. The method is based on the use of silicone oil, which has a low toxicity, unlike other chemicals generally used in the surface modification by other methods. Also, it is widely used in droplet-based microfluidic experiments and available in a variety of viscosities.

BIOS/Lab-on-Chip Group, MESA+ Institute for Nanotechnology, University of Twente, P. O. Box 217, 7500 AE Enschede, The Netherlands. E-mail: j.c.t.eijkel@utwente.nl; Fax: +31 534893595; Tel: +31 534892691

Additionally, simple microchannels of down to 2 μm depth and 60 μm width could be hydrophobized using both liquid-based hydrophobization (ODS or FDTS) and vapour-based hydrophobization (hexamethyldisilazane, HMDS), reported both by the authors and in many literature reports.[44,56,57] Problems however arose when we tried these methods in micro- and nanochannel networks, where at the interface of micro- and nanochannels and also inside nanochannels clogging occurred. Even though clogging could possibly be removed by flushing, it might be difficult to perform in the complex microfluidic network or nanochannels. *Via* our particle-free method, the hydrophobization is more convenient than the conventional methods especially in sub-micron fluidic channels and the complicated fluidic networks.

2. Materials and methods

Glass-based microfluidic devices

Glass-based devices with a micro–nanochannel network were made from a borosilicate glass wafer (Borofloat 33, 4 inch, 1.1 mm thick, Schott Technical Glasses, Germany). To enhance the adhesion of the photoresist, hexamethyldisilazane (HMDS) was first deposited onto the glass wafer in the vacuum oven (150 °C, 5 min). Then, the photoresist was patterned on the glass wafer by standard photolithography and used as a mask for a wet-etching step in buffered hydrofluoric acid (VLSI Selectipur, BASF) for 14 min to create 500 nm deep nanochannels prior to the resist removal by nitric acid. Subsequently, the microfluidic network was fabricated by a similar method as mentioned above with a deposited metal mask of Cr/Au (14/140 nm) for a wet-etching process in 25% hydrofluoric acid (VLSI Selectipur, BASF) for 5 min to obtain 5 μm deep channels. Then, the metal mask and resist were removed before powder blasting holes for fluidic connection. Finally, the patterned substrate was bonded to another 0.5 mm thick borofloat glass wafer using a thermal bonding technique.

Surface modification

Prior to the modification process, the glass chip was cleaned and dehydrated in the oven at 120 °C for 2 h. Subsequently, the chip was activated by oxygen plasma (Harrick Plasma Cleaner, NY, USA), at a pressure of 400 mTorr and a power of 30 W for 10 min. Then, silicone oil (Sigma-Aldrich, The Netherlands) was applied into the fluidic chips using a neMESYS syringe pump (Cetoni, Korbussen, Germany). All types of silicone oil (silicone oil 1, 5, 20 and 50 cSt) were purchased from Sigma-Aldrich, The Netherlands. Fluidic connections were made using fused silica tubing (O.D.: 360 μm) and fluidic connectors purchased from Upchurch Scientific (WA, USA). After filling with silicone oil, the chip was exposed to UV light (680 mW cm^{-2}, Konrad Benda UV-lamp short and long wave UV-8S/L, Germany) with a wavelength of 254 nm. The lamp was placed at a fixed distance (~0.5 cm) from the samples. During UV exposure, the glass chip was immersed into silicone oil to prevent the evaporation of oil. Finally, the glass chip was cleaned by immersing in octane, acetone and isopropanol. Alternatively, a stainless-steel mask was used to confine hydrophobic patterns on the glass chip upon UV exposure. The procedure of the modification approach is illustrated in Fig. 1.

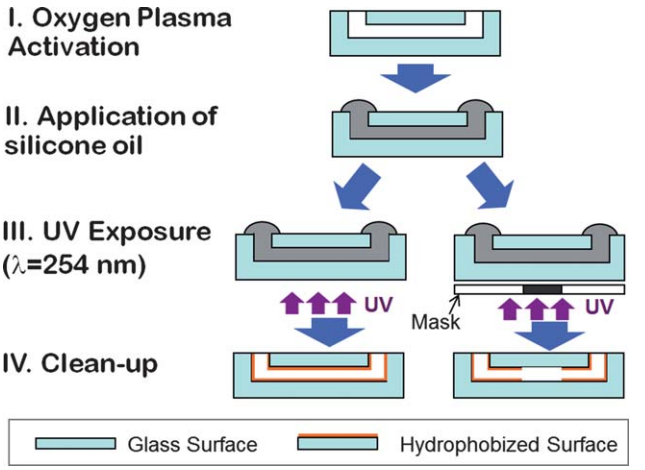

Fig. 1 Schematic diagram of the procedure of the surface modification by using UV-light and the silicone oil.

Characterization

Contact angle measurement. Static contact angle measurement of the outer surface of a glass chip was performed using a Dataphysics System (Dataphysics, OCA20, Germany) in the sessile drop mode using DI water before and after hydrophobization of various modification parameters such as UV-treatment time, and oil type as shown in Table 1, and Fig. 2 and 3. In the first experiment, the samples were treated by oxygen plasma and then exposed to UV light. In the second experiment, samples were irradiated by UV light directly without oxygen plasma treatment. In the third experiment, samples were activated by oxygen plasma, immersed into the oil and then stored in the dark for 2 h instead of being irradiated by UV light. Furthermore, the stability of the modified surface was investigated by immersing the modified samples into different polarity solvents (water, ethanol, acetone, silicone oil, octane) for 24 h and by keeping the modified samples in atmospheric circumstances for 3 weeks. All solvents used in this stability test were purchased from Sigma-Aldrich (The Netherlands).

X-Ray photoelectron spectroscopy (XPS). XPS characterization has been conducted with a monochromatic X-ray beam (Al

Table 1 Contact angle measurements (degree) of glass surfaces before and after modification using different modification approaches[a]

	After modification		
Before modification	O_2(+), UV(+)	O_2(−), UV(+)	O_2(+), UV(−)
31.0 ± 3.9	100.9 ± 2.8	68.2 ± 0.2	89.0 ± 4.0

[a] *Note*: three different approaches of surface modification were carried out: (1) with oxygen plasma [O_2(+)] and with UV exposure [UV(+)]; (2) without oxygen plasma [O_2(−)] and with UV exposure [UV(+)]; (3) with oxygen plasma [O_2(+)] and without UV exposure [UV(−)].

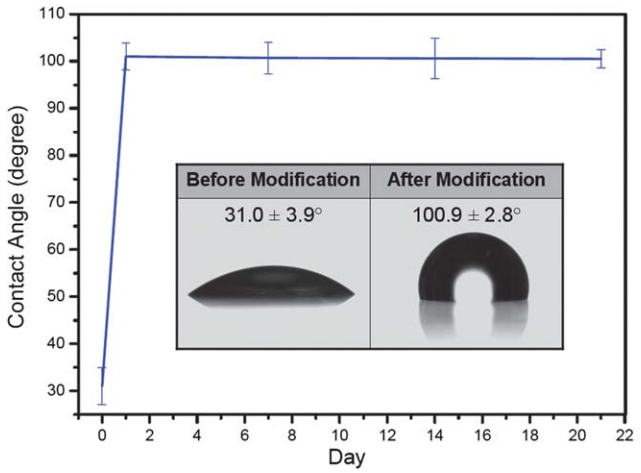

Fig. 2 Contact angle measurement of the outer glass surface before (date 0th) and after modification (after three weeks). Inset: images of water droplet (2 μL) onto the glass surface before and after surface modification.

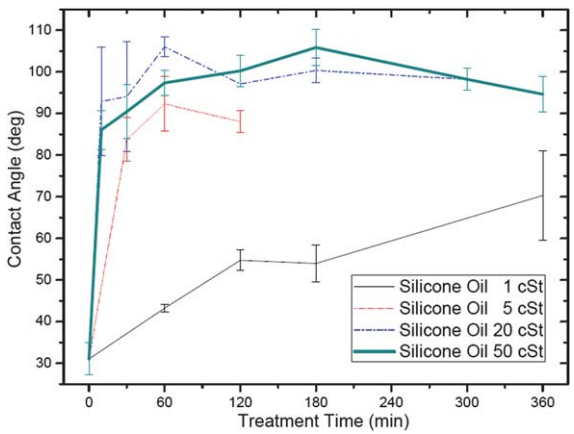

Fig. 3 Contact angle measurement of the outer glass surface at different UV-treatment times (min) and types of silicone oil.

KR, 1486.6 eV, 100 W, Quantera, Physical Electronics). Mapping was done at 3×10^{-9} Torr and detector angles of 70 and 45°. XPS spectra were taken from a bare glass substrate and a modified glass sample.

W/O emulsion generation. The micro- and nanochannel network modified by this approach was used to generate a W/O emulsion. The homogeneity of the surface modification inside the nanochannel sections was observed from the undisturbed flow of water droplets in the oil phase since any unmodified glass surface presented a hydrophilic area on which water droplets would be trapped. The aqueous phase in these experiments was DI water and the oil phase was 0.5 wt% Span80 in hexadecane. The viscosities of water and oil phases were 1 and 3 mPa s, respectively. All chemicals used in fluidic experimentation were bought from Sigma-Aldrich Chemie GmbH (Germany). The video and images were obtained by an inverted microscope (Leica DMIRM) and recorded by a CCD camera (Orca ER) with an Analysis Docu program (Olympus).

Hydrophobic patterning. Hydrophobic areas were patterned both on the plane glass sample and in an enclosed microchannel system using the above-mentioned procedure in combination with an in-house produced stainless steel mask. The UV-exposed area became hydrophobic whereas the unexposed area remained hydrophilic. After modification, on the plane substrate, vaporized water was condensed onto the hydrophobic patterned surface. Different dimensions of condensed droplets expressed the diverse hydrophobicity on the patterned surface.[58] In the enclosed microchannel device, DI water would flow into hydrophilic microchannels by capillary force, but would cease to flow when reaching the hydrophobic area. The magnitude of the additionally applied pressure that would make the water resume its flow through the hydrophobic sector was used to determine the advancing contact angle inside the hydrophobic channel section.

3. Results and discussion

Contact angle

The effects of oxygen plasma and UV exposure on the surface modification were determined from the change in the contact angle of the outer surface of a glass chip. Table 1 gives a comparison of the contact angle of the surface hydrophobized by different processes (with or without O_2 plasma activation and UV exposure steps) when applying silicone oil 50 cSt in combination with two hour UV exposure. It was shown that only one step of either oxygen plasma or UV exposure does enhance the contact angle but to a lesser extent than the combination of both steps (Table 1). The effect of oxygen plasma and UV exposure is discussed in the next section.

In addition, as can be seen from Fig. 2, modification of the glass surfaces by silicone oil 50 cSt in combination with 2 hour UV exposure results in a contact angle of 100° measured from several samples. Additionally, the UV treatment times were varied from 10 min to 6 h to investigate the optimal time for modification (Fig. 3). Three hour curing time proved the optimal condition for silicone oil 50 cSt since the obtained contact angle was the maximum (105.9°). When the sample was treated by UV irradiation for a longer time, the resultant contact angle decreased with higher deviation.

Other types of silicone oil (silicone oil 1, 5 and 20 cSt) were also tested (Fig. 3) showing the same trend of resultant contact angle as a function of treatment time. The optimal curing times were dependent on the type of oils, and the hydrophobic surface modified by silicone oil 50 cSt provided the highest contact angle among these oils. Overexposure was found to heat the oil (temperature increases to 45 °C after 2 h) causing the evaporation of oil or the formation of tiny air bubbles in the oil phase.

X-Ray photoelectron spectroscopy (XPS)

XPS data of unmodified and modified samples are shown in Fig. 4A–D. A survey spectrum of both samples (Fig. 4A) shows the changes in the atomic ratio of each element especially for carbon (C1s), oxygen (O1s) and silicon (Si2p). High-resolution spectra of C1s, O1s and Si2p are individually illustrated in Fig. 4B–D.

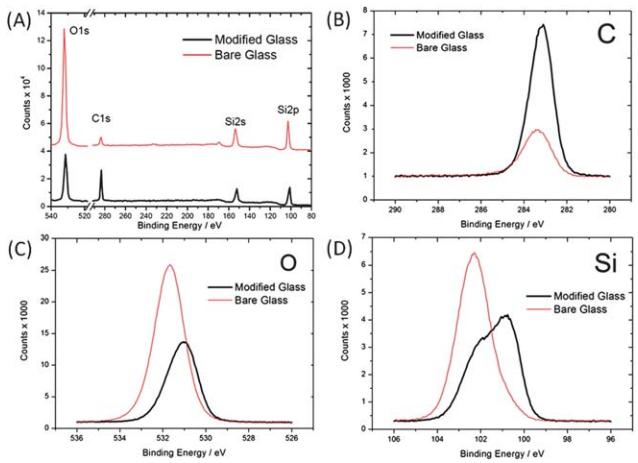

Fig. 4 XPS results of the bare glass and modified glass substrate: (A) survey spectrum, (B) C1s spectrum, (C) O1s spectrum and (D) Si2p spectrum.

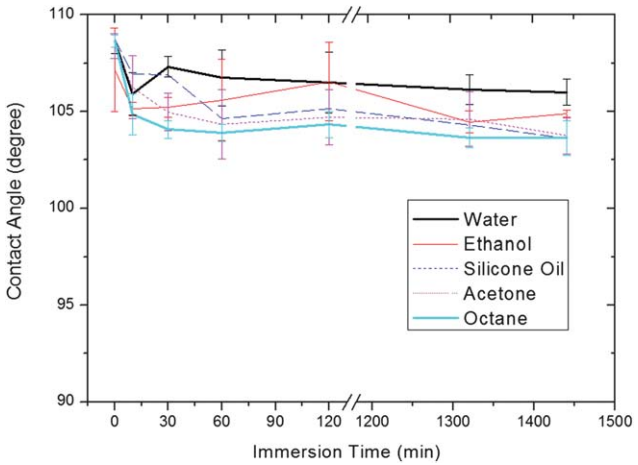

Fig. 5 Stability of the hydrophobized glass surface in several solutions with different polarities until 24 h.

An obvious increase in carbon atoms from 11% to 34% (Fig. 4B and Table 2) was attributed mainly to the formation of fragments of silicone oil molecules. The peak of C1s from the unmodified glass surface might be assigned to the contamination of organic compounds on the surface. In general, the binding energy of O1s in SiO_2 and in hydroxyl groups is 533 and 532 eV, respectively.[59] The shift of binding energy for O1s after modification (Fig. 4C and Table 2) was mainly due to the absence of OH groups resulting from the formation of a silicone oil layer onto the glass surface. The binding energy of Si2p in a silicone oil molecule (Si–C or Si–O bond) and in SiO_2 is 102 and 103 eV, respectively.[59] After hydrophobization, more silicon atoms with a binding energy of 102 eV were observed in the Si2p XPS data as opposed to that from the unmodified sample, verifying that silicone oil molecules were attached onto the glass surface (Fig. 4D and Table 2). The atomic ratios of each element (C1s, O1s, Si2p) and of the shifted binding energy (O1s, Si2p) after modification are shown in Table 2.

Stability

Contact angles of the hydrophobized surfaces measured before and after immersion into various solutions with different polarities (water, ethanol, acetone, octane, and silicone oil) after 24 h are shown in Fig. 5. Also, the contact angles of the samples stored in the atmospheric circumstance were measured after three weeks as illustrated in Fig. 2. After 24 hour immersion into different solutions, the contact angles slightly decreased with a maximum of around 5° (see Fig. 5) and almost remained constant for three weeks in the case of the sample stored in the atmosphere (see Fig. 2). These data indicate the good stability of the hydrophobized surface modified with this approach in different polarity solvents. We interpret the results as showing that the solvents applied can remove a physisorbed layer of silicone oil or organic compounds on the glass surface, but not break covalent bonds of the hydrophobic layer formed at the surface.

Table 2 Atomic ratio of C1s, O1s and Si2p from the XPS results[a]

	Atomic ratio (%)						
Sample	C	O			Si		
Bare glass	11.1	60.5	*532 eV* *96*	*533 eV* *4*	27.9	*102 eV* *4*	*103 eV* *96*
Modified glass	34.3	36.7	*532 eV* *75*	*533 eV* *25*	27.4	*102 eV* *40*	*103 eV* *60*

[a] *Note*: the italic numbers expressing the percentage of each element (O1s and Si2p) at different binding energies.

In-channel modified surface

After hydrophobization, neither particulate debris nor clogging was found in the glass-based micro- and nanofluidic networks, which is especially remarkable inside the nanochannel network (Fig. 6, *left*) and the intersection of micro- and nanochannels, where standard hydrophobization methods tend to cause particle deposition (Fig. 6, *middle*). When water was applied in the microfluidic channel, the advancing contact angle deduced from the meniscus shape was above 90° as shown in Fig. 6, *right*.

Homogeneity (W/O emulsion)

After modification, the modified glass-based chip was used for droplet generation (water-in-oil). The fluidic chip consists of

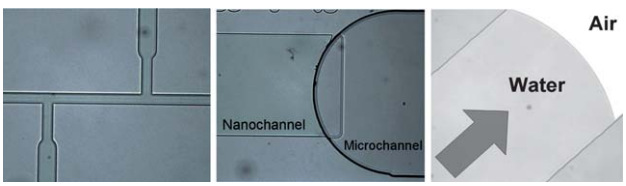

Fig. 6 Micro- and nanofluidic networks after modification. No clogging or formation of particulate debris occurred. [*Left*] Nanochannel network (width: 6 and 8 μm). [*Middle*] Intersection of nano- and microchannels. The widths of the nanochannel and microchannel were 100 and 150 μm, respectively. [*Right*] Meniscus of the water phase against air in the microchannel after surface modification (arrow indicates the flow direction of fluid); the width of the channel was 100 μm. The depths of all nanochannels and microchannels were 500 nm and 5 μm, respectively.

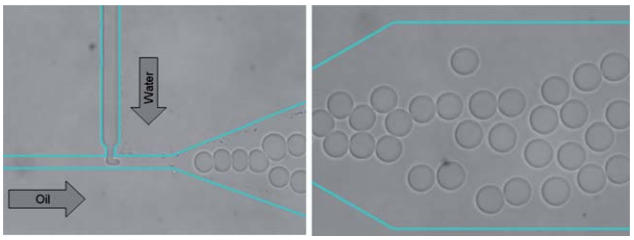

Fig. 7 [*Left*] Water-in-oil droplet formation in a hydrophobized glass chip (the water phase was deionized water and the oil phase was 0.5 wt% Span80 in hexadecane solution), [*right*] generated water-in-oil droplets flowing in the outlet channel without sticking show the homogeneous coating obtained by this method; all channels were 1 μm deep and the widths of the inlet channels and outlet channels were 10 and 100 μm, respectively. The blue lines visualize the confinement of the nanochannel network.

micro- and nanochannel networks with a T-junction of the nanochannels where the tip of the water stream was detached by shear force from the oil stream forming water droplets flowing in a continuous oil phase. Fig. 7 (*left*) shows the successful generation of 50 fL water droplets at the nanochannel T-junction (width: 10 μm, depth: 0.5 μm). When performing this fluidic experiment for a few hours, the formed droplet continuously homogeneously flowed in the nanochannel outlet (width: 10 μm, depth: 0.5 μm) without droplets sticking on the channel wall as illustrated in Fig. 7, *right*. This stands in contrast to cases of inhomogeneous coating, where water droplets would become stuck on hydrophilic surface patches.

Hydrophobic patterning

After illumination incorporated with a metal mask and clean-up, the hydrophobic pattern on a plane glass surface was characterized by exposing the surface to vaporized DI water. The difference in hydrophobicity on the surface then caused different dimensions of condensed droplets on the glass surface.[58] Due to the larger surface energy on the hydrophilic area (the wetting effect of water on a hydrophilic surface), condensed droplets were larger and flatter than those on the hydrophobic area. Flatter droplets on the hydrophilic surface also showed a brighter image than those on the hydrophobic surface as illustrated in Fig. 8.

For the micro- and nanofluidic chip, the hydrophobic patterning was tested in the microchannel section by using the

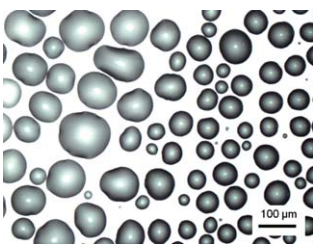

Fig. 8 Patterned hydrophobic surface on a bare glass substrate illustrating the hydrophobized area on the right side and unmodified area on the left side. Vaporized water condensed onto the patterned hydrophobic surface creating smaller droplets due to lower surface energy, on the contrary, larger and flatter droplets condensed onto a hydrophilic glass surface because of a wetting effect.

principle of hydrophobic valving as described earlier in the literature.[51,52] The water phase is wetting on hydrophilic sectors and non-wetting on hydrophobic sectors. In our chip, the sections that are exposed to only oxygen plasma and silicone oil in the experiments on free glass surfaces are expected to be hydrophilic ($\theta < 90°$) while the sections exposed to oxygen plasma, silicone oil and UV light will be hydrophobic ($\theta > 90°$). We indeed observed that after treatment of the channels the water spontaneously but slowly advanced through the section treated with oxygen plasma and silicone oil while it ceased to advance when reaching the border of the sectors treated with oxygen plasma, silicone oil and UV. This process can be described by a model of capillary filling. With a given external pressure, the water subsequently advances through the non-wetting sector. This given pressure is ruled by the water/gas interfacial tension (γ_{wg}), the radius of curvature of the aqueous phase which is related to the height (h) and the width (w) of the fluidic channel, and the advancing contact angle of the hydrophobic surface (θ_{phob}) as shown in the equation:

$$P = -2\gamma_{wg}\frac{h+w}{hw}\cos\theta_{phob} \quad (1)$$

The hydrostatic pressure ($P_{hydrostatic}$) of water as adjusted by the positions of the water reservoir and the microchannel system (ΔH) was used to provide a relatively low pressure to the water as shown in eqn (2) where ρ is the density of water and g is the gravitational acceleration.

$$P_{hydrostatic} = \rho g(\Delta H) \quad (2)$$

In our experiment, the height and the width of the fluidic channel were 5 and 100 μm, respectively, and the surface tension between water and air (γ_{wg}) is ~70 mN m^{-1}. A height difference (ΔH) of around 35 cm was needed to introduce water into the hydrophobic sector. The applied pressure was therefore approximately 34 mbar or 3418 N m^{-2} according to eqn (1) yielding an advancing contact angle of the in-channel hydrophobic surface of about 96.4°.†

Discussion: possible mechanism

The glass surface is first activated by oxygen plasma enabling removal of contaminants such as dust, grease, and organic compounds from the glass surface. Plasma can also enhance the number of hydroxyl terminated groups (OH) on the surface of SiO_2, causing a higher surface energy and decreasing water contact angle.[60] In general, when silicone oil is applied to the glass surface, the oil would physically adsorb onto terminal OH groups on the glass surface due to van der Waals attraction and hydrogen bonds between the oxygen atoms in the polymer backbone and the silanol groups on the glass surface.[61] With oxygen plasma activation, oil was seen to spread out faster than without plasma activation which we interpret as the result of an increasing number of hydroxyl

† To avoid confusion between the contact angle from the hydrophobic valving calculation and the one from the contact angle measurement by a sessile drop method, it is worth mentioning that the contact angle determined from the hydrophobic valving concept is *the advancing contact angle* which is different from *the static contact angle* measured by a sessile drop method.

surface groups. The effect of irradiation on polydimethylsiloxane (PDMS) molecules has been reported earlier in the literature.[62] Silicone oil has the same molecular structure as PDMS. Upon UV exposure, photons from the UV lamp with a wavelength of 254 nm have an energy of 469 kJ mol^{-1} (4.88 eV) which is enough to break some bonds in the silicone oil molecules forming radicals of oil molecules. We propose that these radicals formed diffuse to the surface and react with the hydroxyl groups on the glass surface, leaving the non-polar tails of the oil molecules in contact with the solution forming the hydrophobic surface.

The application of oxygen plasma resulted in a higher contact angle (80°) despite the lack of UV irradiation. This increase was probably due to the effect of oxygen plasma on a hydroxylated silica surface (Si–OH). As mentioned before, the oxygen plasma can remove organic contaminants and break hydrogen bonds between hydroxyl groups (OH) and their neighbouring oxygen atom causing more OH groups on the surface. Furthermore, hydroxylated silica (Si–OH) can form strained edge-shared tetrahedral Si–O–Si bonds by heating at high temperature (above 650 °C)[63] or by oxygen plasma treatment.[64] Dehydroxylated siloxane bonds were reported to have a greatly enhanced reactivity compared to hydroxyl groups on the silica surface.[63–65] This strained form might be highly reactive to silicone oil molecules even without molecular radical formation of oil by UV irradiation.

A long exposure led to a decrease of the observed contact angle and increased the observed deviation. Long exposure times might lead to the creation of a multilayer of oil molecules or the formation of unexpected molecular products. The evaporation of oil or the formation of air bubbles occurring from heating upon UV-overexposure probably inhibited the high surface coverage causing the highly deviated contact angle. From our measurement, after two hour UV irradiation, the silicone oil was heated to a temperature of 45°.

4. Conclusion

In micro- and nanofluidic technology, approaches to hydrophobize in-channel microfluidic systems have rarely been reported. Commonly used modification methods are accomplished in a plane wafer before bonding and/or require skilful handling procedures. Moreover, nanofluidic networks are more problematic for any modification approaches especially with respect to debris left over after modification. In our novel approach, in-channel fluidic networks were hydrophobized by filling with silicone oil in combination with plasma activation and UV irradiation. The treatment can reduce the surface energy resulting in contact angles of 100° or more remaining stably hydrophobic in solvents of different polarities for more than three weeks. Layers were characterized by XPS. Glass-based micro- and nanofluidic chips were successfully modified without the formation of particulate debris, and could be used to produce W/O emulsions verifying the homogeneity of the modified surface. It was finally shown that this method lends itself to selective in-channel hydrophobization by the application of a UV mask.

Acknowledgements

The authors would like to thank all technical supports and particularly Muhammad Nasir Masood in BIOS Group.

References

1 K. Xiao, M. Y. Zhang, S. Y. Chen, L. M. Wang, D. C. Chang and W. J. Wen, *Electrophoresis*, 2010, **31**, 3175–3180.
2 Y. H. Zhan, J. Wang, N. Bao and C. Lu, *Anal. Chem.*, 2009, **81**, 2027–2031.
3 Y. Schaerli and F. Hollfelder, *Mol. BioSyst.*, 2009, **5**, 1392–1404.
4 A. B. Theberge, F. Courtois, Y. Schaerli, M. Fischlechner, C. Abell, F. Hollfelder and W. T. S. Huck, *Angew. Chem., Int. Ed.*, 2010, **49**, 5846–5868.
5 B. Zheng, J. D. Tice and R. F. Ismagilov, *Anal. Chem.*, 2004, **76**, 4977–4982.
6 Y. C. Tan, J. S. Fisher, A. I. Lee, V. Cristini and A. P. Lee, *Lab Chip*, 2004, **4**, 292–298.
7 L. M. Fidalgo, G. Whyte, D. Bratton, C. F. Kaminski, C. Abell and W. T. S. Huck, *Angew. Chem., Int. Ed.*, 2008, **47**, 2042–2045.
8 M. Hashimoto, P. Garstecki and G. M. Whitesides, *Small*, 2007, **3**, 1792–1802.
9 W. H. Tan and S. Takeuchi, *Lab Chip*, 2006, **6**, 757–763.
10 H. Song, J. D. Tice and R. F. Ismagilov, *Angew. Chem., Int. Ed.*, 2003, **42**, 768–772.
11 Y. M. Jung and I. S. Kang, *Biomicrofluidics*, 2010, **4**, 024104.
12 L. L. Shui, A. van den Berg and J. C. T. Eijkel, *Lab Chip*, 2009, **9**, 795–801.
13 P. Abbyad, R. Dangla, A. Alexandrou and C. N. Baroud, *Lab Chip*, 2011, **11**, 813–821.
14 M. Chabert and J. L. Viovy, *Proc. Natl. Acad. Sci. U. S. A.*, 2008, **105**, 3191–3196.
15 J. Clausell-Tormos, D. Lieber, J. C. Baret, A. El-Harrak, O. J. Miller, L. Frenz, J. Blouwolff, K. J. Humphry, S. Koster, H. Duan, C. Holtze, D. A. Weitz, A. D. Griffiths and C. A. Merten, *Chem. Biol.*, 2008, **15**, 427–437.
16 S. Koster, F. E. Angile, H. Duan, J. J. Agresti, A. Wintner, C. Schmitz, A. C. Rowat, C. A. Merten, D. Pisignano, A. D. Griffiths and D. A. Weitz, *Lab Chip*, 2008, **8**, 1110–1115.
17 N. Wu, F. Courtois, R. Surjadi, J. Oakeshott, T. S. Peat, C. J. Easton, C. Abell and Y. G. Zhu, *Eng. Life Sci.*, 2011, **11**, 157–164.
18 V. Chokkalingam, B. Weidenhof, M. Kramer, W. F. Maier, S. Herminghaus and R. Seemann, *Lab Chip*, 2010, **10**, 1700–1705.
19 H. Hwang, S. H. Kim and S. M. Yang, *Lab Chip*, 2011, **11**, 87–92.
20 S. H. Kim, A. Abbaspourrad and D. A. Weitz, *J. Am. Chem. Soc.*, 2011, **133**, 5516–5524.
21 S. H. Kim, S. J. Jeon, G. R. Yi, C. J. Heo, J. H. Choi and S. M. Yang, *Adv. Mater.*, 2008, **20**, 1649.
22 S. H. Kim, J. W. Shim, J. M. Lim, S. Y. Lee and S. M. Yang, *New J. Phys.*, 2009, **11**, 075014.
23 T. Nisisako, T. Torii, T. Takahashi and Y. Takizawa, *Adv. Mater.*, 2006, **18**, 1152.
24 J. Wan, M. Sullivan and H. A. Stone, *Controllable Production of Gas/Water/Oil Double Emulsions in Microfluidic Devices*, 2007.
25 R. M. Lorenz, G. S. Fiorini, G. D. M. Jeffries, D. S. W. Lim, M. Y. He and D. T. Chiu, *Anal. Chim. Acta*, 2008, **630**, 124–130.
26 Y. Liu, S. Y. Jung and C. P. Collier, *Anal. Chem.*, 2009, **81**, 4922–4928.
27 J. C. Baret, F. Kleinschmidt, A. El Harrak and A. D. Griffiths, *Langmuir*, 2009, **25**, 6088–6093.
28 M. Y. He, J. S. Edgar, G. D. M. Jeffries, R. M. Lorenz, J. P. Shelby and D. T. Chiu, *Anal. Chem.*, 2005, **77**, 1539–1544.
29 P. R. Marcoux, M. Dupoy, R. Mathey, A. Novelli-Rousseau, V. Heran, S. Morales, F. Rivera, P. L. Joly, J. P. Moy and F. Mallard, *Colloids Surf., A*, 2011, **377**, 54–62.
30 S. A. Vanapalli, A. G. Banpurkar, D. van den Ende, M. H. G. Duits and F. Mugele, *Lab Chip*, 2009, **9**, 982–990.
31 A. R. Abate, A. Poitzsch, Y. Hwang, J. Lee, J. Czerwinska and D. A. Weitz, *Phys. Rev. E: Stat., Nonlinear, Soft Matter Phys.*, 2009, **80**, 026310.
32 J. J. Agresti, E. Antipov, A. R. Abate, K. Ahn, A. C. Rowat, J. C. Baret, M. Marquez, A. M. Klibanov, A. D. Griffiths and D. A. Weitz, *Proc. Natl. Acad. Sci. U. S. A.*, 2010, **107**, 4004–4009.
33 P. Garstecki, M. J. Fuerstman, H. A. Stone and G. M. Whitesides, *Lab Chip*, 2006, **6**, 437–446.
34 B. Y. Kim, L. Y. Hong, Y. M. Chung, D. P. Kim and C. S. Lee, *Adv. Funct. Mater.*, 2009, **19**, 3796–3803.
35 J. N. Lee, C. Park and G. M. Whitesides, *Anal. Chem.*, 2003, **75**, 6544–6554.

36 R. Dangla, F. Gallaire and C. N. Baroud, *Lab Chip*, 2010, **10**, 2972–2978.
37 J. U. Shim, S. N. Patil, J. T. Hodgkinson, S. D. Bowden, D. R. Spring, M. Welch, W. T. S. Huck, F. Hollfelder and C. Abell, *Lab Chip*, 2011, **11**, 1132–1137.
38 P. Tremblay, M. M. Savard, J. Vermette and R. Paquin, *J. Membr. Sci.*, 2006, **282**, 245–256.
39 J. Lee, Y. K. Yun, Y. Kim and K. Jo, *Bull. Korean Chem. Soc.*, 2009, **30**, 1793–1797.
40 M. M. J. Decre, P. H. M. Timmermans, O. van der Sluis and R. Schroeders, *Langmuir*, 2005, **21**, 7971–7978.
41 K. J. Hsia, Y. Huang, E. Menard, J. U. Park, W. Zhou, J. Rogers and J. M. Fulton, *Appl. Phys. Lett.*, 2005, **86**, 154106.
42 S. M. Park, Y. S. Huh, H. G. Craighead and D. Erickson, *Proc. Natl. Acad. Sci. U. S. A.*, 2009, **106**, 15549–15554.
43 M. Beck, M. Graczyk, I. Maximov, E. L. Sarwe, T. G. I. Ling, M. Keil and L. Montelius, *Microelectron. Eng.*, 2002, **61–62**, 441–448.
44 E. M. Chan, A. P. Alivisatos and R. A. Mathies, *J. Am. Chem. Soc.*, 2005, **127**, 13854–13861.
45 J. Moresco, C. H. Clausen and W. Svendsen, *Sens. Actuators, B*, 2010, **145**, 698–701.
46 Y. X. Zhuang, O. Hansen, T. Knieling, C. Wang, P. Rombach, W. Lang, W. Benecke, M. Kehlenbeck and J. Koblitz, *J. Microelectromech. Syst.*, 2007, **16**, 1451–1460.
47 A. Hibara, M. Nonaka, H. Hisamoto, K. Uchiyama, Y. Kikutani, M. Tokeshi and T. Kitamori, *Anal. Chem.*, 2002, **74**, 1724–1728.
48 X. A. Mu, Q. L. Liang, P. Hu, K. N. Ren, Y. M. Wang and G. A. Luo, *Microfluid. Nanofluid.*, 2010, **9**, 365–373.
49 R. D. Oleschuk, L. L. Shultz-Lockyear, Y. B. Ning and D. J. Harrison, *Anal. Chem.*, 2000, **72**, 585–590.
50 M. Watanabe, *Sens. Actuators, B*, 2007, **122**, 141–147.
51 B. Zhao, J. S. Moore and D. J. Beebe, *Science*, 2001, **291**, 1023–1026.
52 H. Andersson, W. van der Wijngaart, P. Griss, F. Niklaus and G. Stemme, *Sens. Actuators, B*, 2001, **75**, 136–141.
53 Y. Y. Feng, Z. Y. Zhou, X. Y. Ye and H. J. Xiong, *Sens. Actuators, A*, 2003, **108**, 138–143.
54 E. T. Castellana, S. Kataoka, F. Albertorio and P. S. Cremer, *Anal. Chem.*, 2006, **78**, 107–112.
55 T. Vong, J. ter Maat, T. A. van Beek, B. van Lagen, M. Giesbers, J. C. M. van Hest and H. Zuilhof, *Langmuir*, 2009, **25**, 13952–13958.
56 A. Hibara and M. Fukuyama, *Anal. Sci.*, 2011, **27**, 671–672.
57 M. Loughran, S. W. Tsai, K. Yokoyama and I. Karube, *Curr. Appl. Phys.*, 2003, **3**, 495–499.
58 J. ter Maat, R. Regeling, M. L. Yang, M. N. Mullings, S. F. Bent and H. Zuilhof, *Langmuir*, 2009, **25**, 11592–11597.
59 J. F. Moulder, W. F. Stickle, P. E. Sobol and K. D. Bomben, *Handbook of X-Ray Photoelectron Spectroscopy*, Perkin-Elmer Corporation, 1992.
60 T. Yamamoto, M. Okubo, N. Imai and Y. Mori, *Plasma Chem. Plasma Process.*, 2004, **24**, 1–12.
61 K. G. Marinova, D. Christova, S. Tcholakova, E. Efremov and N. D. Denkov, *Langmuir*, 2005, **21**, 11729–11737.
62 S. W. Hu, X. Q. Ren, M. Bachman, C. E. Sims, G. P. Li and N. Allbritton, *Anal. Chem.*, 2002, **74**, 4117–4123.
63 B. C. Bunker, D. M. Haaland, T. A. Michalske and W. L. Smith, *Surf. Sci.*, 1989, **222**, 95–118.
64 R. F. Hicks, S. B. Habib and E. Gonzalez, *J. Vac. Sci. Technol., A*, 2010, **28**, 476–485.
65 A. Grabbe, T. A. Michalske and W. L. Smith, *J. Phys. Chem.*, 1995, **99**, 4648–4654.